

# Aspects Concerning Flame Propagation of Various Fuels in Combustion Chamber of Four Valve Engines

Zoran Jovanovic, Zoran Masonicic, S. Dragutinovic, Z. Sakota

**Abstract**—In this paper, results concerning flame propagation of various fuels in a particular combustion chamber with four tilted valves were elucidated. Flame propagation was represented by the evolution of spatial distribution of temperature in various cut-planes within combustion chamber while the flame front location was determined by dint of zones with maximum temperature gradient. The results presented are only a small part of broader on-going scrutinizing activity in the field of multidimensional modeling of reactive flows in combustion chambers with complicated geometries encompassing various models of turbulence, different fuels and combustion models. In the case of turbulence two different models were applied i.e. standard  $k-\epsilon$  model of turbulence and  $k-\xi-f$  model of turbulence. In this paper flame propagation results were analyzed and presented for two different hydrocarbon fuels, such as CH<sub>4</sub> and C<sub>8</sub>H<sub>18</sub>. In the case of combustion all differences ensuing from different turbulence models, obvious for non-reactive flows are annihilated entirely. Namely the interplay between fluid flow pattern and flame propagation is invariant as regards turbulence models and fuels applied. Namely the interplay between fluid flow pattern and flame propagation is entirely invariant as regards fuel variation indicating that the flame propagation through unburned mixture of CH<sub>4</sub> and C<sub>8</sub>H<sub>18</sub> fuels is not chemically controlled.

**Keywords**—Automotive flows, flame propagation, combustion modelling.

## I. INTRODUCTION

It is known for a long time that various types of organized flows in combustion chamber of IC Engines are of predominant importance for combustion particularly with regards to flame front shape and its propagation. Some results related to the isolated or synergic effect of squish and swirl on flame propagation in various combustion chamber layouts are already analyzed and published [1] but results concerning the isolated or combined effect of the third type of organized flow i.e. tumble are relatively less presented [2]-[4]. From the theory of turbulence is known that vortex filament subjected to compression reduces its length and promotes rotation around its axis yielding the movement on the larger scale ("spin-up" effect). It can be presumed that tumble pursues the same rule i.e. the destruction of formed and expressive tumble during compression stroke generates the higher turbulence intensity and larger integral length scale of turbulence in the vicinity of TDC contributing to the flame kernel formation period reduction and faster flame propagation thereafter [5]. The aforementioned logic imposes the conclusion that the most beneficial fluid flow pattern in the vicinity of BDC is well

shaped high intensity tumble flow.

## II. MODEL AND COMPUTATIONAL METHOD

The analysis of this type is inherent to multidimensional numerical modelling of reactive fluid flow and therefore it is quite logical to apply such a technique particularly due to fact that it is the only technique that encompasses the valve/port geometry layout in an explicit manner. In lieu of the fact that, in its essence, multidimensional models require initial and boundary conditions only their applications is fairly complicated and imply some assumptions and simplifications [6]. The full 3D conservation integral form of unsteady equations governing turbulent motion of non-reactive mixture of ideal gas is solved on fine computational grid with moving boundaries in physical domain by dint of AVL FIRE code [7]. In this case the numerical solution method is based on a fully conservative finite volume approach. For the solution of a recast linear system of equations, a conjugate gradient type of solver (CGS) is used. Two different models of turbulence were used. The first one is nearly forty years old  $k-\epsilon$  model based on Boussinesq's assumption which is, certainly, the most widely used model for engineering computations. The second one is  $k-\xi-f$  model of turbulence i.e. eddy-viscosity model based on Durbin's elliptic relaxation concept [9]-[12]. This model solves a transport equation for the velocity scale ratio  $\xi$  instead of imaginary turbulent normal stress component. In addition, the pertinent hybrid boundary conditions were applied.

## III. RESULTS AND DISCUSSION

### A. Fuel Variation

The analysis of relevant results was based on a fairly complex geometry layout presented in Figs. 1, 2. Obviously, combustion chamber is constrained with dual intake and exhaust valves. The basic block data sheet consists of bore/stroke ratio=80/81.4 mm, squish gap=1.19 mm, engine speed RPM=5500 min<sup>-1</sup> and mixture quality  $\lambda=1$ . In addition, maximum valve lift is 6.95 mm for intake valves and 6.63 mm for exhaust valves while the other geometrical data (relative location, valve shape etc.) could be seen in Figs. 1, 2. It should be stated that results presented in this paper were selected from bunch of results obtained with various models of turbulence, various models of combustion and for different fuels as it is set forth in Table I.

Zoran Jovanovic, Zoran Masonicic, S. Dragutinovic, and Z. Sakota are with the University of Belgrade, Institute "Vinča", Laboratory for IC Engines and Motor Vehicles, Belgrade, Serbia (e-mail: masonicicz@vinca.rs).

TABLE I  
COMBINATION OF FUEL, TURBULENCE AND COMBUSTION MODEL

4-valve engine (Figs. 1 and 2)			
Bore/Stroke	80/81.4 mm		
Rpm	5500 rpm		
Squish gap	1.19 mm		
Mixture quality ( $\lambda$ )	1		
<i>Fuel used</i>	<i>Turbulence model</i>	<i>Combustion model</i>	
Petrol	k- $\xi$ -f	Probability Density Function	
Petrol	k- $\epsilon$	Probability Density Function	
N-octane	k- $\epsilon$	Magnusen-Hjaertager	
N-octane	k- $\xi$ -f	Probability Density Function	
N-octane	k- $\epsilon$	Probability Density Function	
CH4	k- $\epsilon$	Magnusen-Hjaertager	
CH4	k- $\xi$ -f	Probability Density Function	
H2	k- $\epsilon$	Magnusen- Hjaertager	

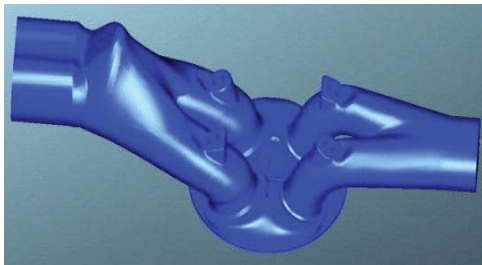


Fig. 1 Perspective view of the combustion chamber geometry layout with 4-valves (top view)



Fig. 2 Perspective view of the chamber geometry layout with 4-valves (bottom view)

The flame propagation through unburned mixture of two different hydrocarbon fuels, such as CH<sub>4</sub> and C<sub>8</sub>H<sub>18</sub>, was analysed by dint of the evolution of spatial distribution of temperatures, represented in form of iso-contours in six cut-planes passing through various parts of combustion chamber geometry layout depicted in Figs. 1 and 2. The flame propagation i.e. the evolution of spatial distribution of temperature in the first cut-plane for C<sub>8</sub>H<sub>18</sub> and CH<sub>4</sub> fuels is shown in Figs. 3-10.

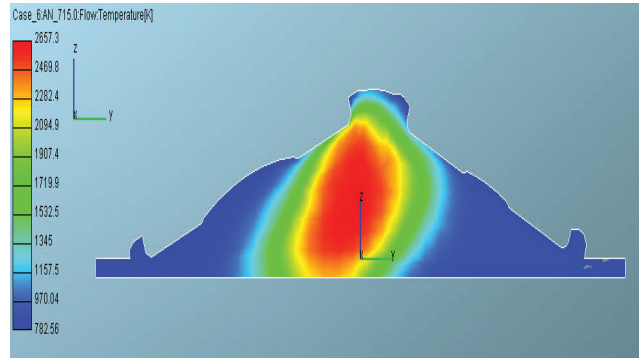


Fig. 3 Spatial distribution of temperature in y-z plane, x=const. at 355 deg. ATDC, k-  $\epsilon$ , C<sub>8</sub>H<sub>18</sub>

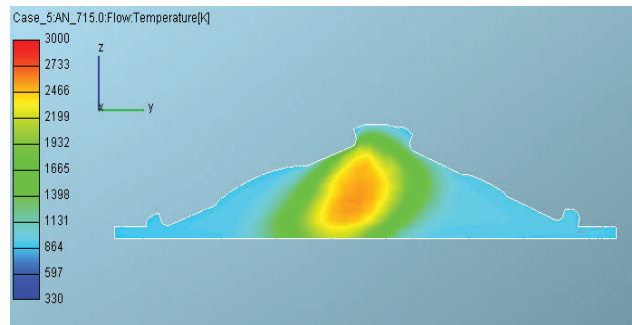


Fig. 4 Spatial distribution of temperature in y-z plane, x=const. at 355 deg. ATDC, k-  $\epsilon$ , CH<sub>4</sub>

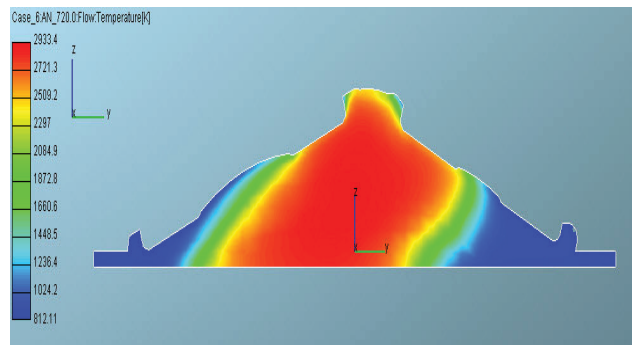


Fig. 5 Spatial distribution of temperature in y-z plane, x=const. at 360 deg. ATDC, k- $\epsilon$ , C<sub>8</sub>H<sub>18</sub>

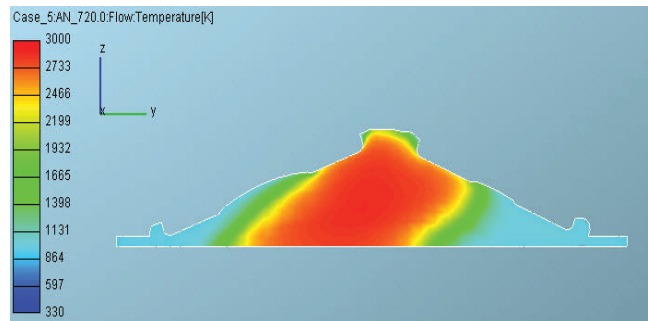


Fig. 6 Spatial distribution of temperature in y-z plane, x=const. at 360 deg. ATDC, k- $\epsilon$ , CH<sub>4</sub>

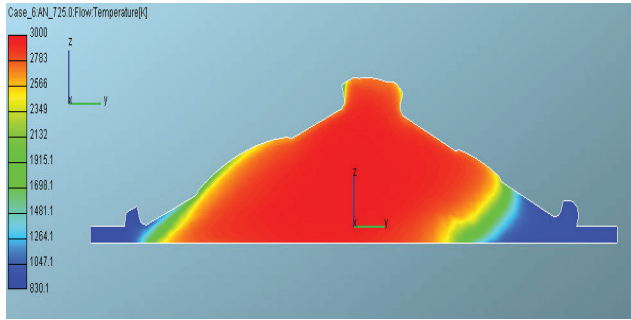


Fig. 7 Spatial distribution of temperature in y-z plane,  $x=const.$  at 365 deg. ATDC,  $k-\epsilon$ , C8H18

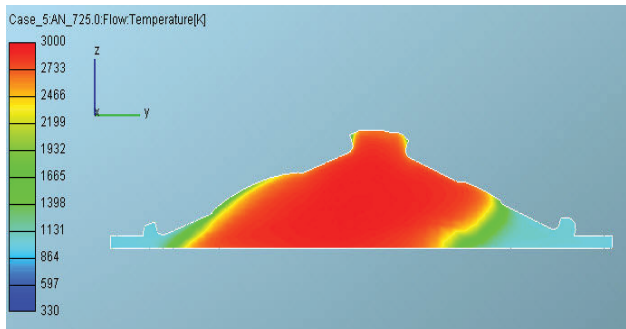


Fig. 8 Spatial distribution of temperature in y-z plane,  $x=const.$  at 365 deg. ATDC,  $k-\epsilon$ , CH4

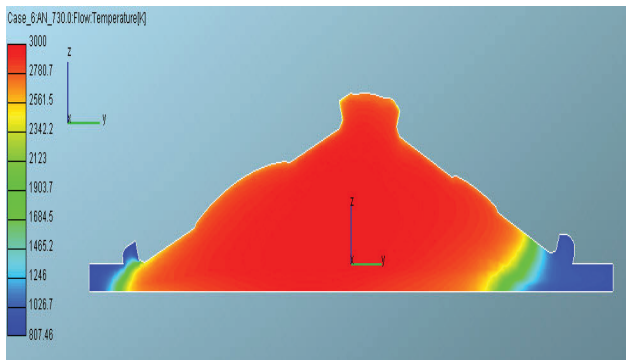


Fig. 9 Spatial distribution of temperature in y-z plane,  $x=const.$  at 370 deg. ATDC,  $k-\epsilon$ , C8H18

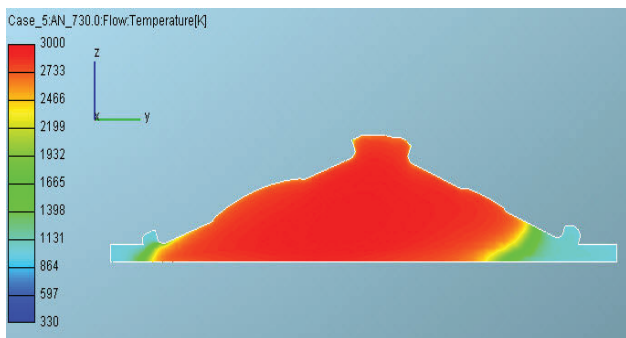


Fig. 10 Spatial distribution of temperature in y-z plane,  $x=const.$  at 370 deg. ATDC,  $k-\epsilon$ , CH4

The flame propagation i.e. the evolution of spatial distribution of temperature in the second symmetry cut-plane for C8H18 and CH4 fuels is shown in Figs. 11-20.

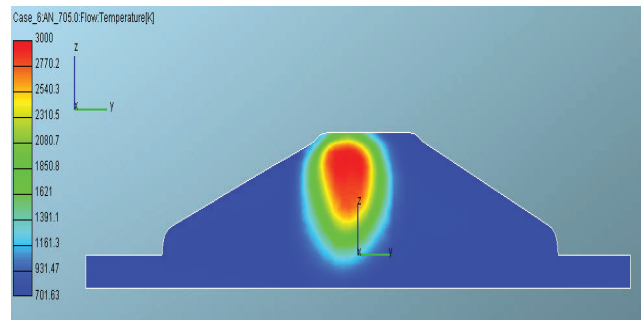


Fig. 11 Spatial distribution of temperature in y-z symmetry plane,  $x=0.0$  at 345 deg. ATDC,  $k-\epsilon$ , C8H18

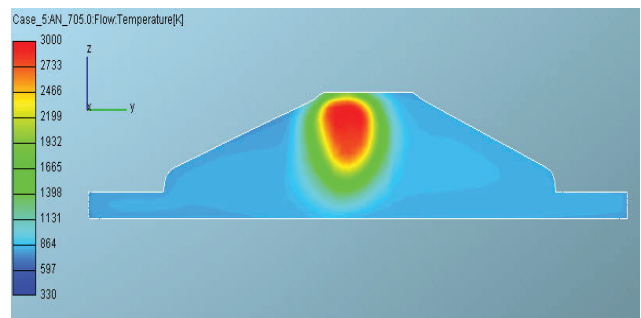


Fig. 12 Spatial distribution of temperature in y-z symmetry plane,  $x=0.0$  at 345 deg. ATDC,  $k-\epsilon$ , CH4

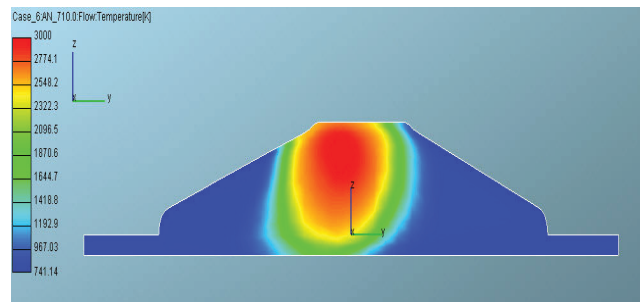


Fig. 13 Spatial distribution of temperature in y-z symmetry plane,  $x=0.0$  at 350 deg. ATDC,  $k-\epsilon$ , C8H18

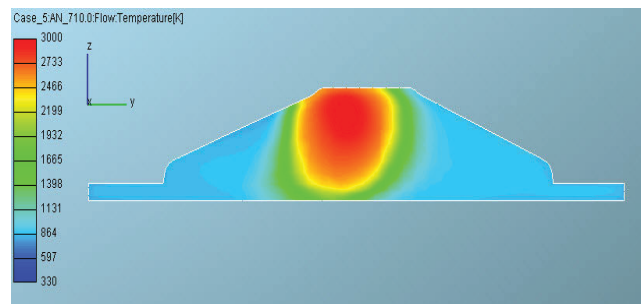


Fig. 14 Spatial distribution of temperature in y-z symmetry plane,  $x=0.0$  at 350 deg. ATDC,  $k-\epsilon$ , CH4

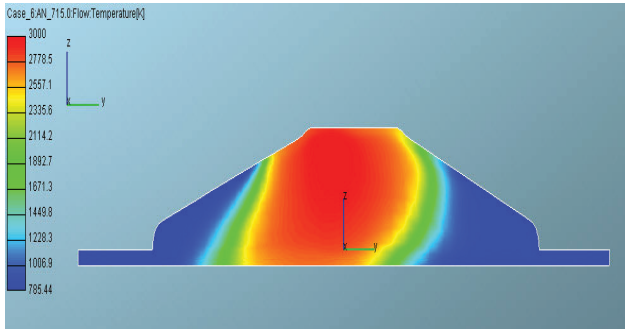


Fig. 15 Spatial distribution of temperature in y-z symmetry plane,  $x=0.0$  at 355 deg. ATDC, k- $\epsilon$ , C8H18

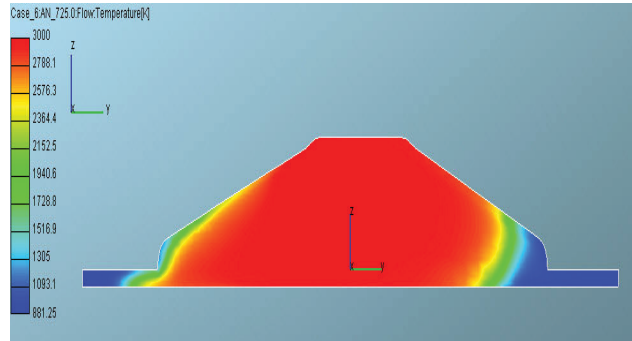


Fig. 19 Spatial distribution of temperature in y-z symmetry plane,  $x=0.0$  at 365 deg. ATDC, k- $\epsilon$ , C8H18

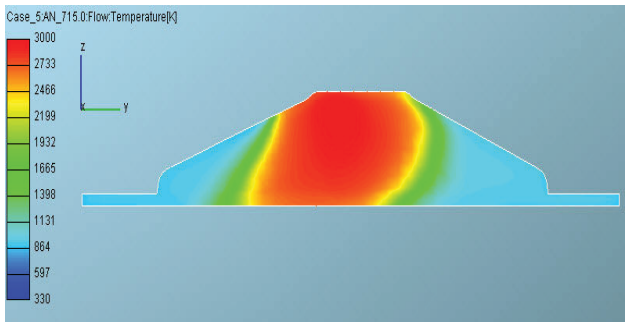


Fig. 16 Spatial distribution of temperature in y-z symmetry plane,  $x=0.0$  at 355 deg. ATDC, k- $\epsilon$ , CH4

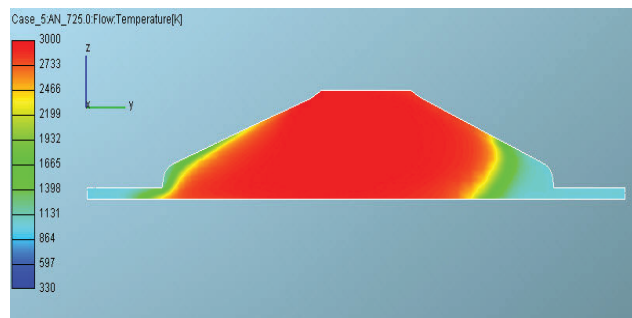


Fig. 20 Spatial distribution of temperature in y-z symmetry plane,  $x=0.0$  at 365 deg. ATDC, k- $\epsilon$ , CH4

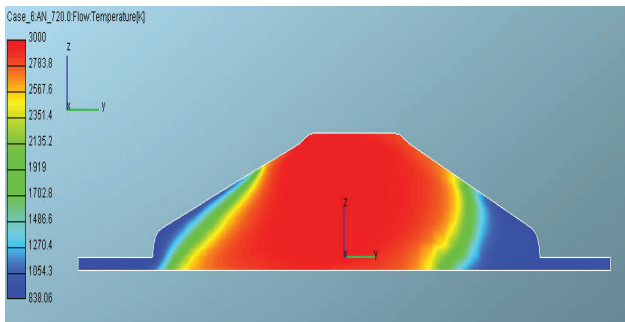


Fig. 17 Spatial distribution of temperature in y-z symmetry plane,  $x=0.0$  at 360 deg. ATDC, k- $\epsilon$ , C8H18

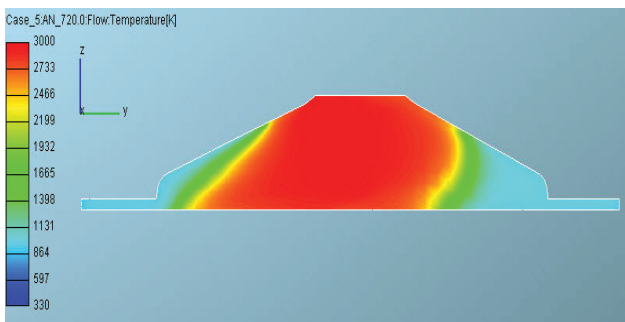


Fig. 18 Spatial distribution of temperature in y-z symmetry plane,  $x=0.0$  at 360 deg. ATDC, k- $\epsilon$ , CH4

The flame propagation i.e. the evolution of spatial distribution of temperature in the sixth cut-plane for C8H18 and CH4 fuels is shown in Figs. 21-30.

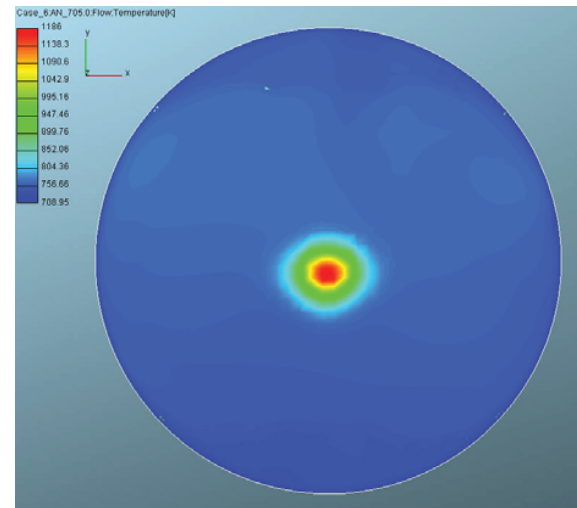


Fig. 21 Spatial distribution of temperature in x-y plane passing through squish zone at 345 deg. ATDC, k- $\epsilon$ , C8H18

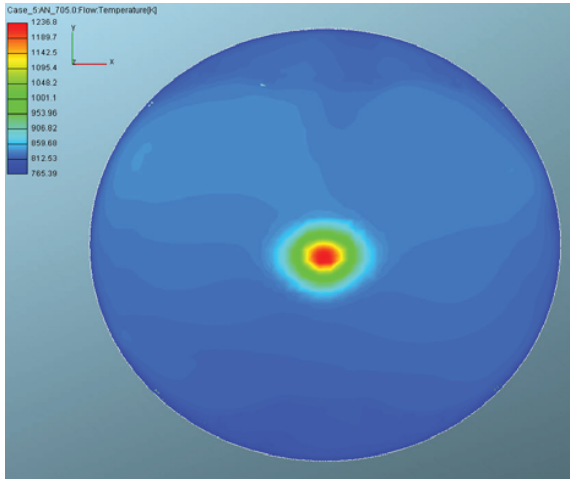


Fig. 22 Spatial distribution of temperature in x-y plane passing through squish zone at 345 deg. ATDC, k-ε, CH4

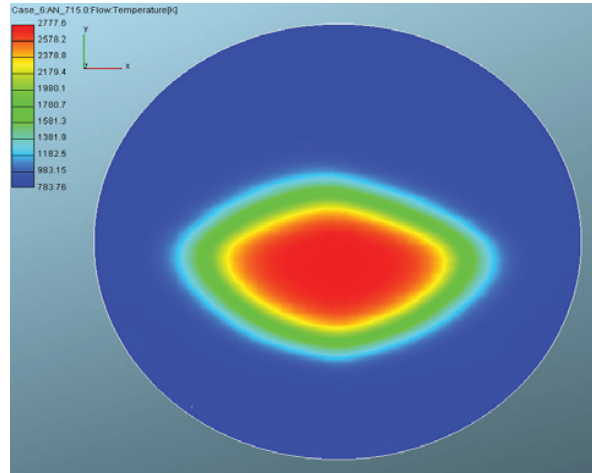


Fig. 25 Spatial distribution of temperature in x-y plane passing through squish zone at 355 deg. ATDC, k-ε, C8H18

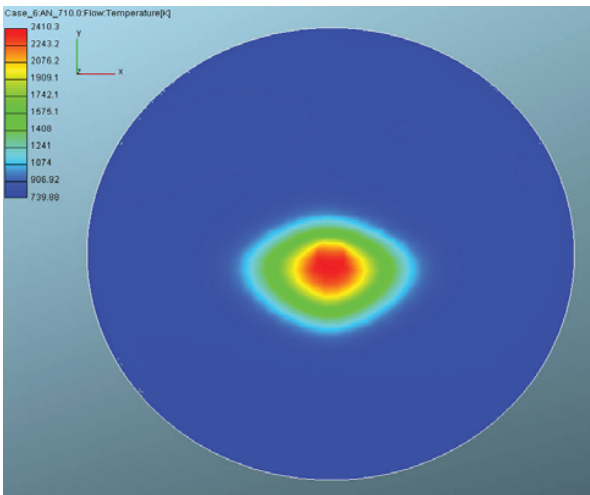


Fig. 23 Spatial distribution of temperature in x-y plane passing through squish zone at 350 deg. ATDC, k-ε, C8H18

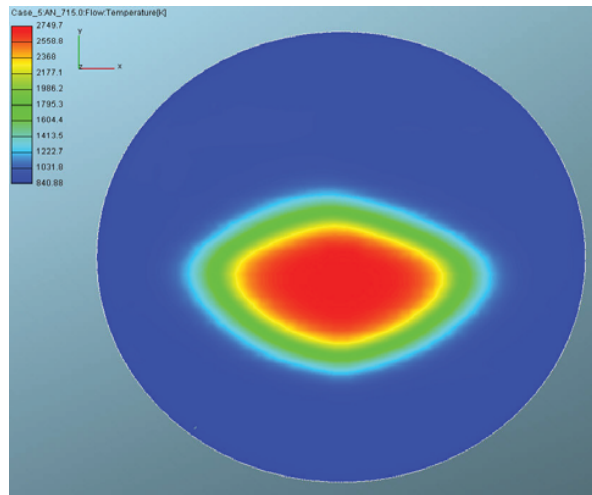


Fig. 26 Spatial distribution of temperature in x-y plane passing through squish zone at 355 deg. ATDC, k-ε, CH4

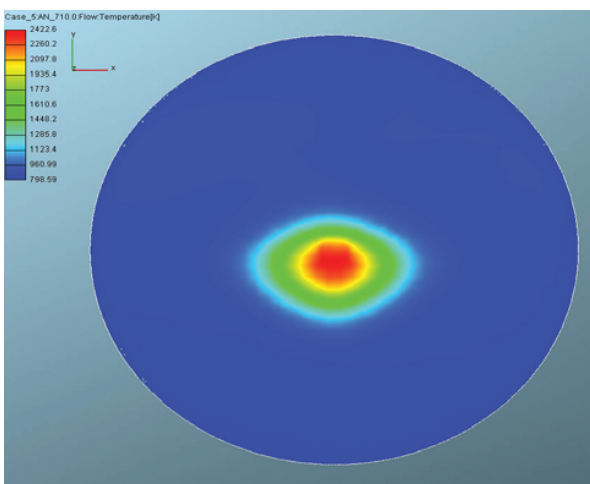


Fig. 24 Spatial distribution of temperature in x-y plane passing through squish zone at 350 deg. ATDC, k-ε, CH4

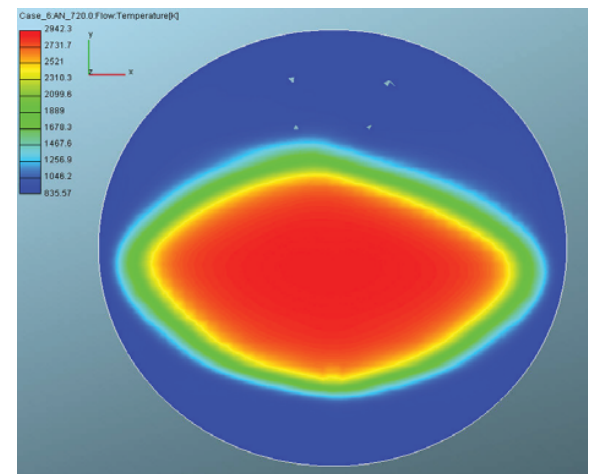


Fig. 27 Spatial distribution of temperature in x-y plane passing through squish zone at 360 deg. ATDC, k-ε, C8H18

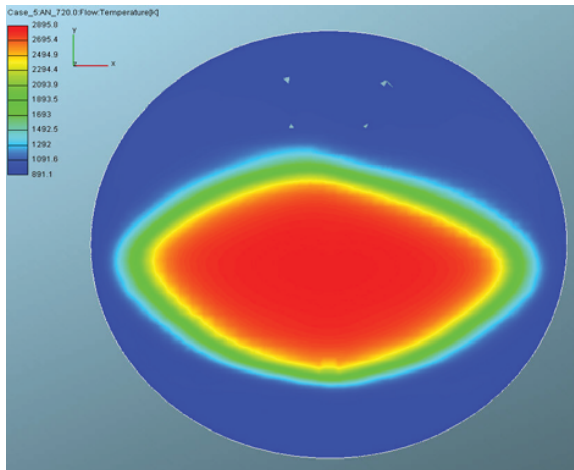


Fig. 28 Spatial distribution of temperature in x-y plane passing through squish zone at 360 deg. ATDC, k- $\epsilon$ , CH4

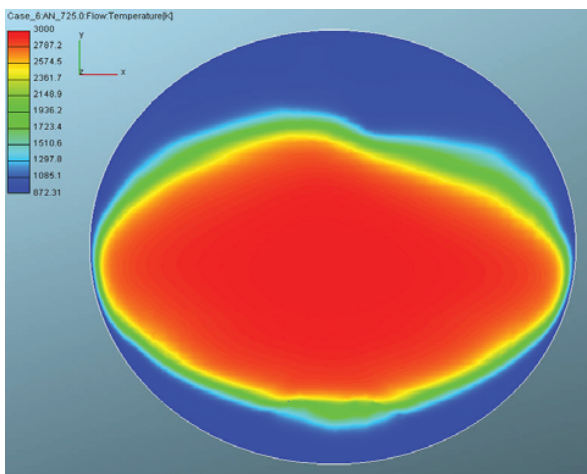


Fig. 29 Spatial distribution of temperature in x-y plane passing through squish zone at 365 deg. ATDC, k- $\epsilon$ , C8H18

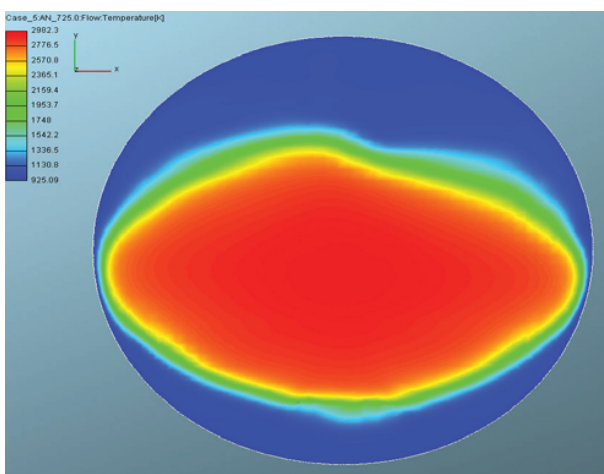


Fig. 30 Spatial distribution of temperature in x-y plane passing through squish zone at 365 deg. ATDC, k- $\epsilon$ , CH4

Obviously, neither differences in flame propagation nor in flame front shape in all cut-planes were encountered for both hydrocarbon fuels used (C8H18 and CH4) yielding the conclusion that flame front shape and its displacement are not chemically controlled but controlled by dint of turbulent diffusion i.e. by high intensity of turbulence and cascade process of tearing or breaking up large vortices into smaller ones and their dissipation into heat.

#### IV. CONCLUSIONS

The fluid flow pattern during induction and compression in the particular combustion chamber geometry of four valve engine is extremely complex and entirely three-dimensional. The modeling of turbulence strongly affects the evolution of fluid flow pattern and spatial distribution of kinetic energy of turbulence in four valve engines. In general k- $\epsilon$  model of turbulence generates higher values of kinetic energy of turbulence over the broader part of the chamber than corresponding k- $\xi$ -f model of turbulence. *In the case of combustion all differences ensuing from turbulence model variation encountered in the case of non-reactive fluid flow are annihilated entirely.* Namely the interplay between fluid flow pattern encountered (“flame dominated fluid flow”) and flame propagation is invariant as regards both turbulence models applied [8]. On the contrary, such a conclusion is not valid either in the case of “squish dominated flows” or in the case of “coincident flow” [1], [2]. The flame front shape and its displacement in IC Engine combustion chamber with strong macro flows are entirely invariant as regards fuel variation tested for both turbulence models indicating that flame propagation is not chemically controlled but controlled by dint of turbulent diffusion. Heat release due to chemical reactions on right hand side of energy equation is of no importance for flame front shape and its displacement presuming that this invariance is valid for broad range of hydrocarbon fuels.

#### REFERENCES

- [1] Z. Jovanovic, S. Petrovic “The mutual interaction between squish and swirl in IC Engines”, (1997), *Mobility and Vehicle Mechanics* 23, 3, 72-86
- [2] Z. Jovanovic, S. Petrovic, M. Tomic “The effect of combustion chamber geometry layout on combustion and emission” (2008) *Thermal Science* vol.12, No.1, pp. 7-24
- [3] K. Lee, C. Baie, K. Kang “The effects of tumble and swirl flows on flame propagation in a four-valve S.I. Engine”, *Applied Thermal Engineering* 27 (2007) 2122-2130
- [4] Ballapu Harshavardhan, J.M. Mallikarjuna “Effect of piston shape on in-cylinder flows and air-fuel interaction in a direct injection spark ignition engine – A CFD analysis” *Energy* 81 (2015) 361-372
- [5] E. A.N. Lipatnikov, J. Chomiak “Effects of premixed flames on turbulence and turbulent scalar transport”, *Progress in Energy and Combustion Science* 36 (2010) 1–102
- [6] Z. Jovanovic “The role of tensor calculus in numerical modeling of combustion in IC engines” *Computer Simulation in Fluid Flow, Heat and Mass Transfer and Combustion in Reciprocating Engines*, Hemisphere Publishers (1989) 457-542, ISBN 0-89116-392-1
- [7] CFD Solver, AVL FIRE 2009.1
- [8] S.L. Yang, Y.K. Siow, C.Y. Teo, K. Hanjalic “A KIVA Code with Reynolds-stress model for engine flow simulation”, *Energy* 30 (2005) 427-445
- [9] P. A. Durbin „Near wall turbulence closure modeling without damping

- functions”, *Theoretical Computational Fluid Dynamics* (1991) 3 1-13
- [10] M. Popovac, K. Hanjalic „Compound wall treatment for RANS computation of complex turbulent flows and heat transfer”, *Flow, Turbulence, Combustion* (2007) 78:177-202
- [11] C.G. Speciale, S. Sarkar, T.B. Gatski “Modelling the pressure strain correlation of turbulence – an invariant dynamical system approach”, pp.1-51, ICASE Report No. 90-5, 1990
- [12] K. Hanjalic, M. Popovac, M. Hadjiabdic „A robust near-wall elliptic relaxation eddy viscosity turbulence model for CFD”, *International Journal of Heat and Fluid Flow*, 25 (2004) 1047-1051